Eur. Phys. J. Plus (2026) 141:574
https://doi.org/10.1140/epjp/s13360-026-07824-0

THE EUROPEAN PHYSICAL JOURNAL PLUS

Regular Article

Near-equilibrium dynamics of the random field Ising model

Gül Gülpınar[1,a], **Songül Özüm**[2,b], **Dicle Yilmaz**[1,c]

[1] Department of Physics, Faculty of Science, Dokuz Eylül University, İzmir 351600, Türkiye
[2] Alaca Avni Celik Vocational School, Hitit University, Çorum 19600, Türkiye

Received: 2 April 2026 / Accepted: 12 May 2026
© The Author(s) 2026

Abstract This study examines the relaxation dynamics of the random field Ising model within a phenomenological framework based on irreversible thermodynamics. A small, uniform external field is applied for a short duration, then suddenly turned off, to monitor the ensuing relaxation of the Ising model under the influence of a longitudinal random field with a distinct bimodal distribution. The mean-field phase diagram is obtained by combining the Landau expansion of the free energy with numerical evaluations of the equations of state. The study shows that the temperature variance of the relaxation time (τ) exhibits singularity near second-order and tricritical points, indicating the well-known critical slowing down phenomena. The relaxation time τ exhibits finite and discontinuous jumps, which is a clear signature of the bimodal random field forcing the system into an abrupt structural shift near a discontinuous phase transition. The critical and tricritical exponents, along with their associated amplitudes, are determined to characterize the system's critical behavior further. A rise in critical amplitude near the tricritical point shows a "flattened" free-energy landscape. This makes the system more sensitive to quenched disorder. The temperature variation of τ reveals the coupled nature of disorder, criticality, and relaxation dynamics in the RFIM.

1 Introduction

Disordered cooperative systems have been a central topic in statistical physics for several decades. Among the theoretical models developed to understand disorder effects, the random field Ising model (RFIM) occupies a prominent position. The RFIM extends the conventional Ising model by including quenched random magnetic fields at each lattice site. Imry and Ma first demonstrated that even weak random fields can destabilize long-range order in low-dimensional systems [1], and subsequent studies by Aharony [2], Nattermann [3], and Fisher [4] highlighted the emergence of tricritical behavior and the complex phase diagram induced by disorder. As a paradigmatic model, RFIM allows the study of the interplay between randomness and cooperative phenomena in many-body systems [2–4]. Experimentally, dilute antiferromagnets in uniform magnetic fields, such as $Fe_xZn_{1-x}F_2$ and $Mn_xZn_{1-x}F_2$, closely realize the RFIM Hamiltonian [5–7]. In these systems, the external field produces effective random fields acting on the magnetic ions, and neutron scattering and magnetization studies have confirmed disorder-induced modifications of critical behavior [5, 8, 9]. Renormalization-group theory identifies a critical fixed point as the basis for the ordering transition in RFIM [10], and related studies explore 3D Gaussian RFIM [11], colloid-polymer mixtures in quenched porous media [12], and random-axis anisotropic magnets [13], demonstrating the broad relevance of the universality class of RFIM. Although the equilibrium properties of the RFIM are extensively investigated, the non-equilibrium dynamics remain an active research area [3, 4, 14, 15]. In disordered systems, relaxation processes slow significantly near phase transitions due to critical slowing, and the characteristic relaxation time τ can diverge. Understanding these dynamics is crucial to interpreting experimental observations and classifying dynamic universality classes. Theoretical frameworks for dynamic critical phenomena were established by Hohenberg and Halperin [16] and by Martin et al. [17], which classify systems such as Model A with non-conserved order parameters. Studies of hysteresis and avalanches also provide insight into non-equilibrium relaxation [18]. Various approaches have been used to study RFIM dynamics. Numerical simulations include cluster-Qipping Monte Carlo [19], Glauber stochastic dynamics [20], effective-field theory [21], and 2D Monte Carlo simulations [22]. Three-dimensional RFIM dynamics under quenched disorder have been explored using Monte Carlo simulations [23], as well as related models, such as the kinetic Ising model under static random fields [24]. The quasi-static magnetizing field has been proposed as a theoretical framework for disordered magnetic systems [25], and recent studies

Gül Gülpınar and Dicle Yilmaz contributed equally to this work.

[a] e-mail: gul.gulpinar@deu.edu.tr
[b] e-mail: songulozum@hitit.edu.tr (corresponding author)
[c] e-mail: dydicleyilmaz@gmail.com

Published online: 22 May 2026

also analyze nucleation dynamics in the random 3D Ising model [26]. Although the relaxation dynamics of the RFIM have been extensively studied using stochastic approaches such as Glauber dynamics and Monte Carlo simulations, these methods primarily yield numerical insights into the system's behavior. In contrast to the extant numerical literature, the present work employs a phenomenological framework rooted in irreversible thermodynamics to derive a closed-form analytical expression for the relaxation time. This analytical approach enables direct mapping of the effects of quenched bimodal disorder on relaxation kinetics across different phase transition regimes, providing a more transparent perspective on the underlying dynamics than purely simulation-based studies. Also, despite extensive research on the equilibrium phase diagram of the RFIM, there has been a paucity of work on the behavior of τ across different types of phase transitions. Of particular interest is the relation between the relaxation dynamics and phase transitions of different natures. In this work, we analyze the relaxation dynamics of RFIM within the framework of irreversible thermodynamics. The system's response to a pulse-like external magnetic field is examined, and the time evolution of the magnetization is used to determine the characteristic time τ within the framework of the equilibrium theory of cooperative phenomena. A similar approach has been used to analyze random Blume–Capel models in a crystal field with different probability distributions [27, 28]. The phase diagram of the RFIM is obtained through Landau analysis and numerical solutions of the equation of state, while first-order phase transitions (FOPTs) are identified via free-energy minima. Our results indicate that τ diverges near second-order phase transitions (SOPTs) and the tricritical point (TCP), consistent with critical slowing down. In contrast, it remains finite but exhibits a discontinuous jump at FOPTs. The temperature dependence of τ for fixed values of the random field is illustrated in the τ - T curves, which clearly distinguish dynamic behavior between different types of phase transitions. These findings provide insight into the interplay between quenched disorder, phase transitions, and near-equilibrium relaxation dynamics in the RFIM.

2 Model formulation and equilibrium analysis in the mean-field framework

The Hamiltonian for the Ising model under a uniform and random magnetic fields may be defined as follows

$$\mathcal{H} = -J \sum_{\langle i,j \rangle} s_i s_j - \sum_i (h_i + H) s_i, \tag{1}$$

In this expression, $s_i = \pm 1$, J denotes the exchange coupling, and H stands for the uniform magnetic field, while the random fields h_i follow a symmetric bimodal distribution.

$$P(h_i) = \frac{1}{2}\delta(h_i - h_0) + \frac{1}{2}\delta(h_i + h_0), \tag{2}$$

where h_0 characterizes the width of the discrete bimodal probability distribution. Thermal fluctuations are neglected, and each spin interacts with the average magnetization of its neighbors in the mean-field approximation (MFA). The magnetization is defined as

$$m = \langle s_i \rangle. \tag{3}$$

Replacing neighboring spins by m, the effective Hamiltonian becomes

$$\mathcal{H}_i^{\mathrm{MF}} = -s_i (Jzm + h_i + H), \tag{4}$$

where the coordination number is denoted by z. The corresponding single-site partition function reads

$$Z_i(h_i) = \sum_{s_i = \pm 1} \exp[\beta s_i (Jzm + h_i + H)] = 2\cosh\beta(Jzm + h_i + H), \tag{5}$$

where $\beta = 1/(k_B T)$. For quenched disorder, the free energy per site is defined as

$$f = -\frac{1}{\beta}\overline{\ln Z_i(h_i)} + \frac{1}{2}Jzm^2, \tag{6}$$

where the overbar denotes configurational averaging over the random field distribution. Performing the bimodal average yields

$$f = \frac{1}{2}Jzm^2 - \frac{1}{2\beta}\Big[\ln 2\cosh\beta(Jzm + H + h_0) + \ln 2\cosh\beta(Jzm + H - h_0)\Big]. \tag{7}$$

Minimization of the free energy with respect to the order parameter yields the self-consistency equation

$$m = \frac{1}{2}[\tanh(Km + h + h_e) + \tanh(Km - h + h_e)]. \tag{8}$$

Introducing dimensionless parameters

$$K = \beta J z, \qquad h = \beta h_0, \qquad h_e = \beta H, \tag{9}$$

Assuming a zero uniform external field ($H = 0$),

$$m = \frac{1}{2}[\tanh(Km + h) + \tanh(Km - h)]. \tag{10}$$

To assess the extent of local ordering caused by random fields, the spin-glass order parameter q is introduced:

$$q = \frac{1}{2}\left[\tanh^2(Km + h) + \tanh^2(Km - h)\right]. \tag{11}$$

To analyze the phase transition, we expand f near the critical point for small magnetization. Thus, magnetic free energy is formulated according to the Landau functional [2]:

$$\Phi(m) = \Phi_0 + \frac{a_2}{2}m^2 + \frac{a_4}{4}m^4 + \frac{a_6}{6}m^6 + \mathcal{O}(m^8). \tag{12}$$

The Landau coefficients are

$$a_2 = 1 - K(1 - \tanh^2 h_0), \tag{13}$$

$$a_4 = \frac{K^3}{3}(1 - 3\tanh^2 h_0), \tag{14}$$

with $a_6 > 0$. The SOPT line is determined by $a_2 = 0$, $a_4 > 0$. At the tricritical point $a_2 = 0$, $a_4 = 0$, and $a_6 > 0$ [29].

2.1 Magnetic relaxation

We now discuss the near-equilibrium dynamics of the bimodal RFIM, focusing on the irreversible process when a small perturbation slightly removes the system from equilibrium. A standard approach involves applying a weak longitudinal H to induce a minor perturbation from the equilibrium state. The free energy per spin in any near-equilibrium state will be [30]

$$f(m, T, H) = f(m_0, T, H_0) + \Delta f, \tag{15}$$

In this context, $f(m_0, T, H_0)$ represents the per-spin equilibrium free energy, with Δf being the free-energy production due to the variance of the uniform external field from its equilibrium value $\delta H = H - H_0$. The resulting fluctuation of the order parameter $\delta m = m - m_0$. Consequently, free energy moves away from a minimum, and a finite change of free energy (Δf) arises. In the near-equilibrium regime, a Taylor expansion of f about its equilibrium configuration is appropriate. Here, $m = m(t)$ is a dynamical parameter and H is a control parameter. Following the standard quadratic expansion in irreversible thermodynamics [30].

$$\Delta f = \frac{1}{2}[\Gamma(m - m_0)^2 + 2\Pi(m - m_0)(H - H_0) + \Psi(H - H_0)^2 + \Omega(H - H_0)], \tag{16}$$

where Γ, Π, Ψ, and Ω are phenomenological coefficients. The coefficients for free-energy production in Eq. 16 are derived as follows:

$$\begin{aligned}
\Gamma &= 1 + \frac{1}{2T}\left[-2 + \tanh\eta^2 + \tanh\kappa^2\right],\\
\Pi &= \frac{1}{2T}\left[-2 + \tanh\eta^2 + \tanh\kappa^2\right],\\
\Psi &= \frac{1}{2T}\left[-2 + \tanh\eta^2 + \tanh\kappa^2\right],\\
\Omega &= -\frac{1}{2}\tanh\eta - \frac{1}{2}\tanh\kappa,
\end{aligned} \tag{17}$$

Here, $\eta = Km + h + h_e$, $\kappa = Km - h + h_e$. If one makes use of Eq. 10 and Eq. 11 Γ, Π, Ψ and Ω can be expressed in terms of ferromagnetic and spin-glass parameters of RFIM as below:

$$\begin{aligned}
\Gamma &= \frac{T + q - 1}{T},\\
\Pi &= \frac{q - 1}{T},\\
\Psi &= \frac{q - 1}{T},\\
\Omega &= -m.
\end{aligned} \tag{18}$$

At this point, the definition of the generalized force becomes necessary.

$$X_m = \frac{d\Delta f}{d(m - m_0)} = \Gamma(m - m_0) + \Pi(H - H_0), \tag{19}$$

Within the framework of irreversible thermodynamics, the magnetization m undergoes relaxation toward its equilibrium state m_0:

$$\dot{m} = -\frac{\delta m}{\tau}, \tag{20}$$

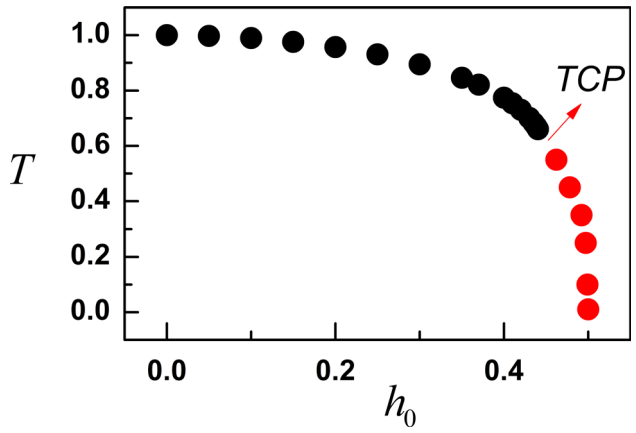

Fig. 1 Phase boundaries in the (T, h_0) plane, showing the evolution of the system's ordered and disordered phases. The arrow denotes the TCPs

where τ characterizes the relaxation behavior of RFIM. Eq. 20 can also be expressed as $\dot{m} = LX$. Here, L signifies the phenomenological rate constant, and X acts as the generalized force conjugate to the rate $\dot{m}$. The generalized force X is defined as the gradient of the free-energy production Δf with respect to the excess magnetization $\delta m = m_t - m_0$. According to the linearized theory, the rate of change for δm_t can be formulated as follows:

$$\frac{d\delta m}{dt} = L\Gamma\delta m - L\Pi H, \tag{21}$$

To derive the relaxation time τ, Eq. 21 is evaluated under the condition $H = H_0 = 0$; subsequently, an ansatz for the deviation δm is postulated in the form:

$$\delta m = m_1 e^{-t/\tau}, \tag{22}$$

where m_1 is the amplitude. Thus, the τ reads

$$\tau^{-1} = -L\Gamma, \tag{23}$$

Finally, one obtains

$$\tau = \frac{T}{L - LT - Lq}. \tag{24}$$

3 Results

In this section, the system's relaxation dynamics are presented in detail and subsequently discussed. The critical and multicritical behavior of the RFIM of a quenched bimodal random magnetic field is investigated using two complementary approaches. First, the Landau coefficient analysis is employed; second, the equation of state is numerically solved. The results obtained allow for the determination of the nature of the phase transitions and the construction of the corresponding phase diagram. Moreover, the occurrence of a FOPT is confirmed by the free-energy minimization. The temperature dependence of the ferromagnetic order parameter and the τ is also analyzed to examine the system's dynamical critical behavior. This study focuses on the effects of quenched bimodal disorder, which has been shown to lead to the emergence of FOPTs and a TCP that is absent in the pure system. Simultaneously, this disorder lowers T_c. Throughout this section, the equilibrium value of the uniform magnetic field is taken to be zero ($H_0 = 0, k_B = 1$). Figure 1 illustrates the phase surface in the $T - h_0$ plane for the RFIM. The black circles correspond to the FOPT, while the red circles denote the SOPT. Finally, the red arrow represents the TCP. It has been observed that, as h_0 increases, T initially increases and subsequently decreases significantly. In particular, a reduction in the phase transition temperature is evident for larger values of h_0.

Figure 2 displays the isothermal f as a function of h_0 near the first-order critical point. As shown in Figure 2, all datasets within the investigated isothermal f range (approximately -0.574 to -0.568) for $T = 0.4524$ exhibit a consistent, statistically significant decreasing trend. The h_0 range is approximately $0.447 - 0.456$ over the field interval considered. The intersection point indicated by a red dot whose projection to the h_0 axis denotes the value of the random field at which the FOPT occurs, while $T = 0.4524$.

Our study employed an approach that combines equilibrium theory with irreversible thermodynamics, identical to the Model A dynamics [30]. To verify the validity of the analysis, the magnetization versus T and spin-glass versus T curves were analyzed. Since magnetization is the key parameter that determines the order in this model, the τ was analyzed by treating the time-dependent change in magnetization as the generalized flux and the increase in free energy as the generalized force. Therefore, the phase curve was obtained and is presented in this section of the paper. Figures 3(a) and 3(b) illustrate the T dependence of the order parameters

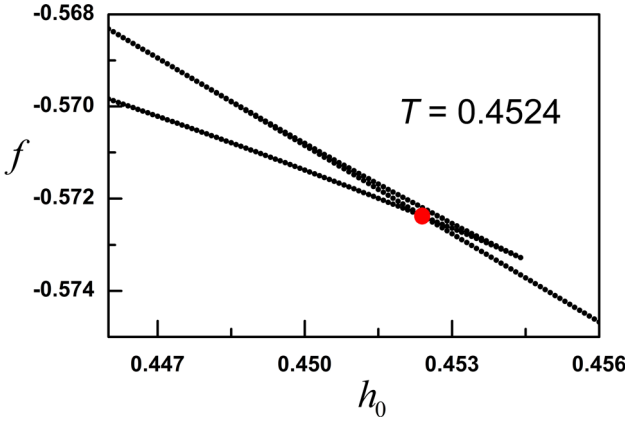

Fig. 2 Isothermal free energy f versus random field h_0 for $T = 0.4524$

(m and q), and Figure 3(c) presents the T evolution of the τ near the SOPT region in a ferromagnetic system described within the MFA. Magnetization m, as a function of dimensionless T, for two values of the reduced external field, $h_0 = 0.41$ (black curve) and $h_0 = 0.20$ (red curve), is presented in Figure 3(a). Both curves exhibit a continuous decrease in m with increasing T, indicative of a second-order ferromagnetic phase transition. Both m and q decrease with increasing T, and the T of the SOPT increases with decreasing h value. For the lower field ($h_0 = 0.20$), a sharper transition region is observed, with m dropping more abruptly toward zero. Magnetization approaches zero value ($m \to 0$) with increasing T. That is, critical behavior of the form $m \sim (T_c - T)^{\beta}$ is observed. Therefore, a SOPT from ferromagnetic to paramagnetic is observed. As illustrated in Figure 3(b), the spin-glass parameter displays a cusp-like behavior at the T_c, suggesting a continuous (SOPT) spin-glass transition. In this regime, the magnetization smoothly decreases to zero as $T \to T_c$, reflecting the gradual loss of frozen spin correlations and the continuous emergence of the spin-glass phase. Unlike the pure Ising model, where $q = m^2$ and both vanish simultaneously at T_c, in our RFIM model, q remains finite even in the paramagnetic phase ($T > T_c$). This phenomenon is attributed to the local pinning effect of the quenched random fields. Despite the loss of long-range ferromagnetic order ($m = 0$), individual spins still partially align with their local fields h_i, resulting in a non-zero value for $q = \langle s_i^2 \rangle$ at higher temperatures. The variation of τ as a function of T for three different random field values ($h_0 = 0.41$ (black), $h_0 = 0.30$ (blue), and $h_0 = 0.20$ (red)) is shown in Figure 3(c). The pronounced peaks in τ are observed in the T interval $0.8 - 1.0$, indicating dramatically slowed dynamics ($\tau \to \infty$) in the vicinity of the phase transition or the coexistence region. The peak position shifts to higher T and becomes narrower as h_0 decreases, suggesting that lower fields lead to stronger critical slowing down near the critical phase transition. Our findings regarding the critical behavior of τ exhibit strong quantitative agreement with previous investigations of iron-group dihalides, specifically those employing ORT phenomenological theory to the antiferromagnetic Ising model with uniform magnetic field, and the Blume–Capel model with quenched disorder due to diluted and fluctuating random crystal fields [28, 31, 32].

As illustrated in Figures 4(a) and (b), m and q are plotted against the temperature for two different values of $h = 0.4563$ (black curve) and 0.493 (red curve). It is evident that both curves decrease with increasing T across the displayed range ($0.20 \leq T \leq 0.40$), and a finite jump of m and q has been observed at the FOPT. For the larger random field, the FOPT temperature increases, as indicated by the black curves in Figures 4(a) and (b). Figure 4(b) shows a sudden jump in q at the transition temperature (denoted T_t). This behavior suggests a FOPT, in which the system undergoes an abrupt onset of finite spin-glass order. The discontinuity observed in q signifies a rapid reconfiguration of the free-energy landscape and the emergence of metastable states. In Fig. 4c, the relaxation time τ is illustrated as a function of temperature T in the vicinity of the FOPT for $h_0 = 0.4563$ and $h_0 = 0.493$. The vertical-dotted lines denote the first-order transition temperatures (T_t) for each random field magnitude. In accordance with the nature of the FOPT, the characteristic relaxation time remains a finite jump at $T = T_t$. These observations exhibit excellent agreement with the results reported in Ref. [28, 33].

In Figures 5(a) to 5(c), the dashed vertical line denotes the location of the T_{tcp}. Figure 5(a) depicts the T variance of the ferromagnetic order parameter for a fixed value of $h_0 = 0.4389$. The symbol T_{tcp} denotes the emergence of first- and second-order phase transition lines. Figure 5(b) depicts the variation of the q as a function of T. The spin-glass parameter exhibits a decrease that is approximately linear in nature with increasing T, thereby reflecting a progressive reduction in the spin-glass ordering of the system. As the parameter T approaches the T_{tcp}, the magnitude of q decreases significantly, indicating that the system approaches a disordered state. Figure 5(c) corresponds to the τ-T curve when $h_0 = 0.4389$. As the T approaches the T_{tcp}, the τ increases dramatically and exhibits a sharp divergence. This divergence is indicative of critical slowing down, a phenomenon in which the system requires progressively longer times to reach equilibrium near the critical point. Beyond the T_{tcp}, τ decreases again as the system moves away from the critical region.

Critical exponents enable the analytical derivation of relaxation time behavior near phase transition points. It is widely recognized that numerous thermodynamic functions exhibit singularities as the critical point is approached; thus, it is advantageous to calculate the dynamical critical exponent z for RFIM. As shown in Figure 6(a), the linear trend on the double-logarithmic scale corroborates the

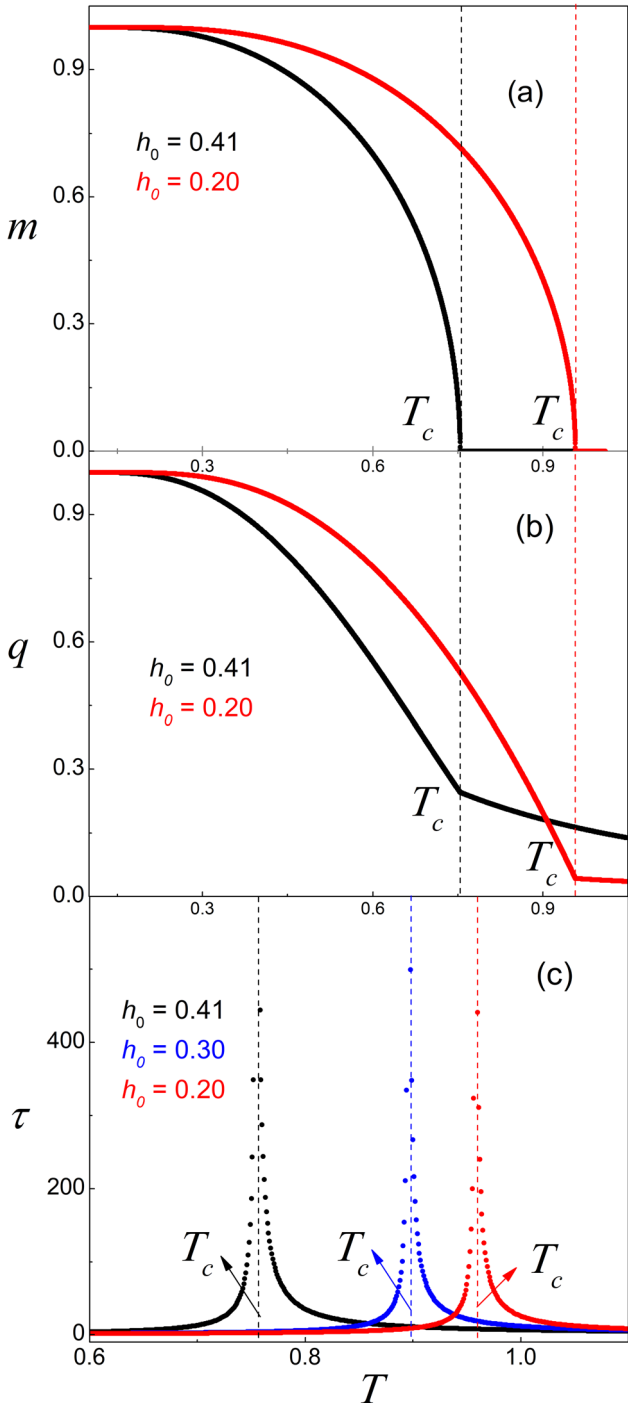

Fig. 3 **a** Magnetization (m), **b** spin-glass order parameter (q), and **c** the relaxation time (τ) as a function of T for a continuous phase transition for different random field (h_0) values. The numbers on the figures correspond to random quenched magnetic field values

algebraic scaling of τ as the $T \to T_c$. RFIM exhibits critical slowing down near SOPTs in which long-range correlations develop, and the system takes longer to return to equilibrium after a perturbation. The slope of the fitted line, approximately -1.00183, indicates that τ scales as $\tau \sim |\epsilon|^{-1}$, yielding a dynamic exponent combination $z\nu \approx 1$, consistent with conventional critical dynamics. Near the TCP, τ also follows a power-law scaling, with a fitted slope of -1.00106 in Figure 6(b). This small deviation reflects subtle changes in relaxation mechanisms due to the coexistence of FOPT and SOPT features, though the overall scaling remains close to an inverse-power-law form. The dynamic scaling of τ near the transition is expressed as $\tau = A_c \cdot \epsilon^{-\nu z}, \quad \epsilon = |T - T_c|/T_c$, where A_c is the critical amplitude and νz is the combined dynamic scaling exponent. Within MFA, adopting $\nu = 1/2$ and $z = 2$ yields the theoretical prediction $\nu z = 1$ [29]. The extracted scaling exponent $z\nu \approx 1$ (consistent with $z \approx 2$ and $\nu = 1/2$ in MFA) characterizes the transition's universality class in the mean-field framework. However, I would like to point out that, for the RFIM, the upper critical dimension is $dc = 6$. In systems with $d < 6$, such as three-dimensional magnets, the mean-field approximation is known to

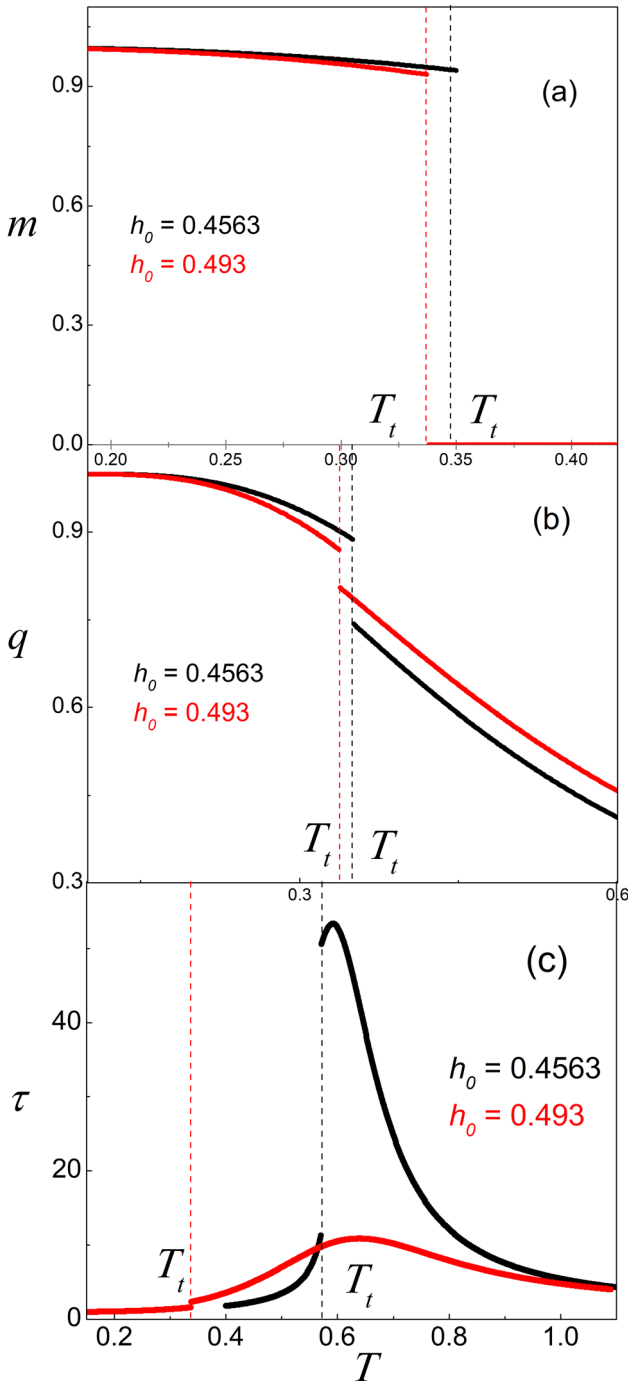

Fig. 4 **a** m, **b** q, and **c** τ as a function of T for a discontinuous phase transition for $h_0 = 0.4563$, 0.493 values

be problematic because it neglects the significant role of critical fluctuations and the effects of dimensional reduction. Consequently, while our extracted exponent is robust within the MFA regime, it should be viewed as an idealized limit. In real-space disordered systems, these exponents may shift significantly as the system enters the Ginzburg region, where the mean-field description typically breaks down. The Ginzburg criterion defines the threshold ϵ_G for the validity of this approximation [34], with $\epsilon_G \propto 1/(\Delta C \cdot \xi_0^d)^2$, where ΔC is the specific heat jump, ξ_0 is the correlation length amplitude, and d is the spatial dimension. In the RFIM, quenched randomness shifts the upper critical dimension d_u due to dimensional reduction effects [3, 35]. Near the TCP, where the fourth-order Landau term vanishes, the scaling regime is modified [36], resulting in a reduced Ginzburg region compared to the standard SOPT. Our numerical analysis, based on self-consistent mean-field equations, accurately describes the system for $\epsilon \gg \epsilon_G$. The calculated exponent $\nu z \approx 1.00$ confirms the robustness of the MFA in capturing universal scaling [37]. Additionally, the increase in critical amplitude from $A_{c,\mathrm{SOPT}} = 0.6245$ to $A_{c,\mathrm{TCP}} = 1.0240$ reflects the "flatter" free-energy landscape at the TCP, indicating enhanced

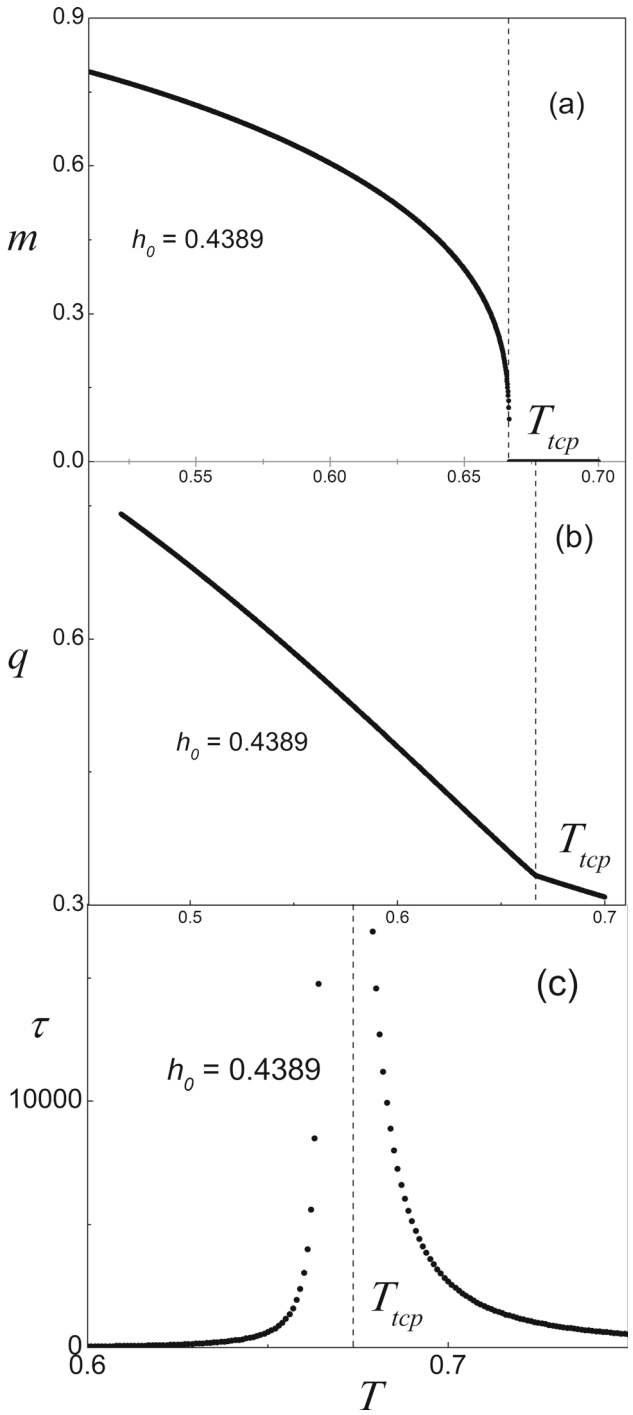

Fig. 5 **a** m, **b** q, and **c** τ as a function of T near the tricritical point for $h_0 = 0.4389$

sensitivity of the relaxation dynamics to the random field distribution as the stabilizing effect of the fourth-order Landau term diminishes.

4 Conclusion

The central contribution of this study is the derivation of the analytical formula for the relaxation time, as presented in Eq. (23). This formula effectively characterizes the critical slowing down near the second-order and tricritical points, obviating the need for extensive computational sampling. Furthermore, the analysis identifies a significant increase in the critical amplitude as the system approaches the tricritical point. This numerical and analytical signature is definitive of the 'flattened' free-energy landscape,

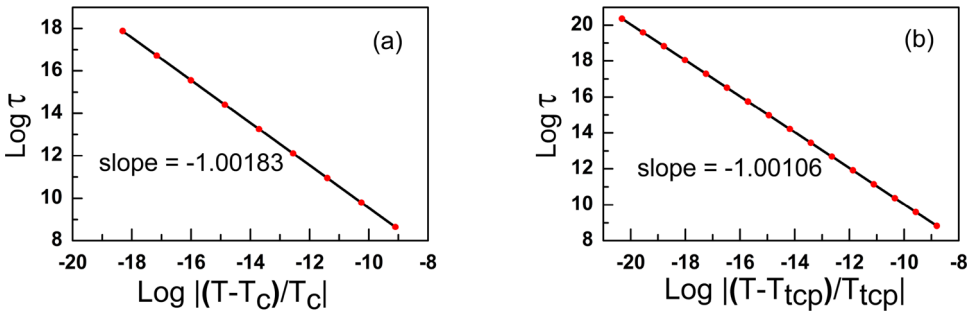

Fig. 6 Log–log plots of the τ as a function of the reduced control parameter for two different critical regimes. **a** log τ versus log $|(T - T_c)/T_c|$ near the critical point T_c. **b** log τ versus log $\left|(T - T_{tcp})/T_{tcp}\right|$ in the vicinity of T_{tcp}. The straight-line behavior in both panels indicates a power-law divergence of the τ, $\tau \sim |\epsilon|^{-z\nu}$, where ϵ is the reduced temperature-like parameter. Red circles represent numerical data, while solid lines denote linear fits used to extract the dynamic critical exponents

a feature that distinguishes the bimodal RFIM's dynamic response from that of other disordered systems. The present work provides an idealized backbone for relaxation processes, thus offering a foundational reference for interpreting dynamical heterogeneity in more complex real-space disordered magnets. The relaxation dynamics of the Ising model with a quenched random field are studied using an approach based on equilibrium theory and irreversible thermodynamics. The model's free energy is obtained via MFA, and its minimization condition yields the self-consistency equation for the ferromagnetic order parameter (m). The phase diagram is given in the (h_0, T) plane for vanishing uniform field ($H_0 = 0$). The results show that the random field induces FOPTs, generates a TCP, and lowers the critical temperature T_c relative to the pure system. The phase diagram of the RFIM displays both SOPTs and FOPTs, separated by a TCP, due to the quenched random field. Assuming that the uniform field is rapidly changed from its equilibrium value and then turned off, the free-energy production by Taylor expansion in terms of equilibrium values of ferromagnetic order parameter and uniform field (m_0, H_0) for constant random field amplitude, h_0. Defining the generalized force and flux in terms of irreversible thermodynamics, the kinetic equation for the ferromagnetic order parameter is derived using linear response theory. Solving the kinetic equation yielded a single characteristic relaxation time that governs the RFIM's relaxation dynamics. Particular attention is devoted to the effects of a quenched bimodal random field on the critical behavior of the Ising model in the neighborhood of the equilibrium. The temperature dependence of the characteristic relaxation time is examined for SOPTs, FOPTs, and the tricritical point. We should note that the relaxation dynamics within MFA are governed by the spin-glass order parameter q. In the vicinity of the critical point, representing the freezing of local spins due to random fields, a critical slowdown emerges. Unlike the pure case, this coupling between m and q in the bimodal RFIM leads to a nonlinear regime where τ reflects metastable states and deeper free-energy wells. The τ exhibits power-law divergences: $\tau \sim |T - T_c|^{-\nu z_c}$ and $\tau \sim |T - T_{tcp}|^{-\nu z_{tcp}}$, respectively . Log-log analysis allows precise extraction of these exponents, yielding $z_c = z_{tcp} \approx 2.0$. Thus, even though the thermodynamic response exponents vary between the critical and tricritical points, shifting from $\beta = 1/2$, $\gamma = 1$, $\delta = 3$ to $\beta = 1/4$, $\gamma = 1$, $\delta = 5$, the metric exponents governing the length and time scales remain invariant at their Gaussian limits, $\nu = 1/2$ and $z = 2$. This distinction explicitly demonstrates that, while the system's thermal-intensity scaling laws are sensitive to the character of the phase transition, the underlying geometric and dynamical scaling remains robust. However, the mean-field results provide the idealized limit in which local relaxation processes converge to a single divergent timescale. Furthermore, the shift in the upper critical dimension for the RFIM highlights the limitations of the MFA approach. While our numerical analysis accurately captures the system in the asymptotic limit where the reduced temperature ϵ is far from the Ginzburg threshold ϵ_G, the interplay between quenched disorder and spatial fluctuations in $d < 6$ may lead to deviations from the $z \approx 2$ behavior predicted here. Future studies that incorporate renormalization group methods or large-scale Monte Carlo simulations would be instrumental in mapping these deviations as the system moves beyond the mean-field 'idealized backbone'. In real disordered systems, the energy landscape is rugged, leading to a broad distribution of local relaxation times, often captured experimentally by the Kohlrausch–Williams–Watts stretched exponential, $\phi(t) = \exp(-(t/\tau_0)^{\beta})$, with $0 < \beta < 1$ [38, 39]. β decreases near the continuous phase transition points, signaling enhanced dynamical heterogeneity. Our findings locate T_c and T_{tcp} through the divergence of τ, consistent with the idealized mean-field picture. Theoretical parallels established with metamagnetic models further reinforce the consistency of our findings for the RFIM with a symmetric bimodal random field. Although both models display identical exponents within the MFA framework, the higher upper critical dimension of the RFIM ($d_{uc} = 6$) makes it inherently more sensitive to dimensional reduction and fluctuation-driven deviations. Nevertheless, the Van Hove linear response characteristic observed in our simulations, along with the value of $z \approx 2$ confirmed by log-log analysis, validates the efficacy of the MFA framework in describing global relaxation processes in bimodal systems. In conclusion, the invariance of dynamical exponents across this complex phase structure indicates that topological relaxation mechanisms exhibit consistent scaling behavior across different transition regimes within the mean-field framework. Although these results demonstrate a degree of independence from the details of bimodal disorder in MFA, we acknowledge that in systems below the upper critical dimension ($d < 6$), the specific characteristics of the disorder could lead to deviations from this universal behavior. It should be noted that the perceived universality in our extracted exponents ($z\nu \approx 1$) arises from the phenomenological thermodynamics approach applied to a mean-field model. In more realistic scenarios, particularly

in three-dimensional disordered magnets, the interplay between random field strength and spatial fluctuations may give rise to different scaling regimes. Therefore, the 'universal' character discussed here should be interpreted as an asymptotic property of the mean-field relaxation dynamics rather than a global claim for all disordered systems. The findings provide a robust theoretical foundation, suggesting that critical slowing down in disordered systems can be evaluated within the same dynamic universality class, regardless of the specific type of phase transition. Our findings are in line with previously published studies on the relaxation dynamics of BC models and the metamagnetic Ising model [27, 28, 32]. Despite the well-known limitations of the MFA, these results still provide a useful starting point for future studies employing more advanced approaches, such as kinetic Monte Carlo simulations, Langevin-based (Model A/B) dynamics, non-equilibrium relaxation methods, and parallel tempering techniques, which can capture relaxation behavior and complex non-equilibrium effects more realistically.

Funding Open access funding provided by the Scientific and Technological Research Council of Türkiye (TÜBİTAK).

Data availability The data supporting the findings of this study are available from the corresponding author upon reasonable request.

Open Access This article is licensed under a Creative Commons Attribution 4.0 International License, which permits use, sharing, adaptation, distribution and reproduction in any medium or format, as long as you give appropriate credit to the original author(s) and the source, provide a link to the Creative Commons licence, and indicate if changes were made. The images or other third party material in this article are included in the article's Creative Commons licence, unless indicated otherwise in a credit line to the material. If material is not included in the article's Creative Commons licence and your intended use is not permitted by statutory regulation or exceeds the permitted use, you will need to obtain permission directly from the copyright holder. To view a copy of this licence, visit http://creativecommons.org/licenses/by/4.0/.

References

1. Y. Imry, S.-K. Ma, Random-field instability of the ordered state of continuous symmetry. Phys. Rev. Lett. **35**, 1399 (1975)
2. A. Aharony, Tricritical points in systems with random fields. Phys. Rev. B **18**, 3318–3327 (1978)
3. T. Nattermann, Theory of the Random Field Ising Model, in Spin Glasses and Random Fields, 277–298, *edited by A* (P. Young, World Scientific, Singapore, 1998)
4. D.S. Fisher, Random fields, random anisotropies, nonlinear σ models, and dimensional reduction. Phys. Rev. B **31**, 7233 (1985)
5. R.J. Birgeneau, H. Yoshizawa, R.A. Cowley, G. Shirane, H. Ikeda, Random-field effects in the diluted two-dimensional Ising antiferromagnet $Rb_2Co_{0.7}Mg_{0.3}F_4$. Phys. Rev. B **28**, 1438–1446 (1983)
6. R. A. Cowley, R. J. Birgeneau, G. Shirane, H. Yoshizawa, Disorder, Random Fields and Competing Interactions in Antiferromagnets, in Multicritical Phenomena, NATO ASI Series, vol 106, edited by R. Pynn and A. Skjeltorp, Springer, Boston, MA (1991)
7. D.P. Belanger, A.P. Young, The random field Ising model, Journal of Magnetism and Magnetic Materials, **100**, 272–291 (1991), North-Holland
8. H. Yoshizawa, R.A. Cowley, G. Shirane, R.J. Birgeneau, Neutron scattering study of the effect of a random field on the three-dimensional dilute Ising antiferromagnet $Fe_{0.6}Zn_{0.4}F_2$. Phys. Rev. B **31**, 4548–4557 (1985)
9. V. Jaccarino, A.R. King, Random exchange and random field Ising systems: static and dynamic critical behavior. Phys. A **163**, 291–305 (1990)
10. D.S. Fisher, Scaling and critical slowing down in random-field Ising systems. Phys. Rev. Lett. **56**, 416–419 (1986)
11. P.E. Theodorakis, I. Georgiou, N.G. Fytas, Fluctuations and criticality in the random-field Ising model. Phys. Rev. E **87**, 032119 (2013)
12. R.L.C. Vink, K. Binder, H. Löwen, Critical behavior of colloid-polymer mixtures in random porous media. Phys. Rev. Lett. **97**, 230603 (2006)
13. M. Dudka, R. Folk, Yu. Holovatch, G. Moser, Critical slowing down in random anisotropy magnets. Condens. Matter Phys. **8**, 737–748 (2005)
14. J.P. Sethna, K.A. Dahmen, C.R. Myers, Crackling noise. Nature **410**, 242–250 (2001)
15. H. Rieger, Critical behavior of the three-dimensional random-field Ising model: two-exponent scaling and discontinuous transition. Phys. Rev. B **52**, 6659–6667 (1995)
16. P.C. Hohenberg, B.I. Halperin, Theory of dynamic critical phenomena. Rev. Mod. Phys. **49**, 435–479 (1977)
17. P.C. Martin, E.D. Siggia, H.A. Rose, Statistical dynamics of classical systems. Phys. Rev. A **8**, 423–437 (1973)
18. K. Dahmen, J.P. Sethna, Hysteresis, avalanches, and disorder-induced critical scaling: a renormalization-group approach. Phys. Rev. B **53**, 14872–14905 (1996)
19. M.E.J. Newman, G.T. Barkema, Monte Carlo study of the random field Ising model. Phys. Rev. E **53**, 393–403 (1996)
20. G. Paula, W. Figueiredo, Dynamical phase diagram of the random field Ising model. Eur. Phys. J. B **1**, 519–522 (1998)
21. E. Costabile, J.R. de Sousa, Phase transitions in a three-dimensional kinetic spin-1/2 Ising model with random field: Effective-field-theory study. Phys. Rev. E **85**, 011121 (2012)
22. S. Sinha, P.K. Mandal, Dynamical properties of random-field Ising model. Phys. Rev. E **87**, 022121 (2013)
23. L. Roters, A. Hucht, S. Lübeck, U. Nowak, K.D. Usadel, Depinning transition and thermal fluctuations in the random-field Ising model. Phys. Rev. E **60**, 5202 (1999)
24. I. Vilfan, Dynamics of the random field Ising model. Solid State Commun. **54**, 795–798 (1985)
25. R. Gozdur, Study of quasi-static magnetization with the random-field Ising model. Algorithms **13**(6), 134 (2020)
26. L. Yao, R.L. Jack, Heterogeneous nucleation in the random field Ising model. J. Chem. Phys. **159**, 244110 (2023)
27. G. Gülpınar, F. Iyikanat, Dynamics of the Blume-1 Capel model with quenched diluted single ion anisotropy in the neighborhood of equilibrium states. Phys. Rev. E **83**, 041101 (2011)
28. S. Özüm, E. Sünnetci, G. Gülpınar, R. Erdem, Relaxation dynamics near the order-disorder and order-order phase transitions in random crystal field Blume-Capel model. Chin. J. Phys. **96**, 461–471 (2025)
29. A. Aharony, Critical behavior of amorphous magnets. Phys. Rev. B **12**, 1038–1048 (1975)
30. J.H. Barry, Magnetic relaxation near a second-order phase-transition point. J. Chem. Phys. **45**, 4172–4177 (1966)
31. S. Özüm, Phenomenological dynamics of Ising magnets in the presence of magnetic field: widom lines captured from slow relaxation time. Acta Phys. Pol., A **140**, 252 (2021)
32. G. Gülpınar, D. Demirhan, F. Buyukkilic, Relaxation dynamics of iron-group dihalides. Phys. Rev. E **75**, 021104 (2007)
33. G. Gülpınar, M. Ağartıoğlu, S. Özüm, Critical relaxation of the (1, 2)-mixed spin Ising model with different single-ion anisotropies. Eur. Phys. J. Plus **140**, 1092 (2025)

34. V.L. Ginzburg, Some remarks on phase transitions of the second kind and the microscopic theory of ferroelectric materials. Sov. Phys. Solid State **2**, 1824–1834 (1960)
35. G. Grinstein, Ferromagnetic phase transitions in random fields: the breakdown of scaling laws. Phys. Rev. Lett. **37**(14), 944–947 (1976)
36. I.D. Lawrie, S. Sarbach, Theory of Tricritical Points, in *Phase Transitions and Critical Phenomena*, C. Domb and J. L. Lebowitz, Eds., vol. 9, pp. 1–161, Academic Press (1984)
37. D.P. Belanger, Experiments on the Random Field Ising Model, in *Spin Glasses and Random Fields*, A. P. Young, Ed., pp. 251–275, World Scientific (1997)
38. R. Kohlrausch, Theorie des elektrischen Rückstandes in der Leidener Flasche. Ann. Phys. **167**, 56–82 (1854)
39. G. Williams, D.C. Watts, Non-symmetrical dielectric relaxation behaviour arising from a simple empirical decay function. Trans. Faraday Soc. **66**, 80–85 (1970)